The Human Kidney Low Affinity Na^+/glucose Cotransporter SGLT2

Delineation of the Major Renal Reabsorptive Mechanism for D-Glucose

Yoshikatsu Kanai, Wen-Sen Lee, Guofeng You, Dennis Brown,* and Matthias A. Hediger

*Renal Division, Department of Medicine, Brigham and Women's Hospital and Harvard Medical School, Boston, Massachusetts 02115; and *Renal Unit and Department of Pathology, Massachusetts General Hospital, Harvard Medical School, Boston, Massachusetts 02114*

Abstract

The major reabsorptive mechanism for D-glucose in the kidney is known to involve a low affinity high capacity Na^+/glucose cotransporter, which is located in the early proximal convoluted tubule segment S1, and which has a Na^+ to glucose coupling ratio of 1:1. Here we provide the first molecular evidence for this renal D-glucose reabsorptive mechanism. We report the characterization of a previously cloned human kidney cDNA that codes for a protein with 59% identity to the high affinity Na^+/glucose cotransporter (SGLT1). Using expression studies with *Xenopus laevis* oocytes we demonstrate that this protein (termed SGLT2) mediates saturable Na^+-dependent and phlorizin-sensitive transport of D-glucose and α-methyl-D-glucopyranoside (αMeGlc) with K_m values of 1.6 mM for αMeGlc and ~ 250 to 300 mM for Na^+, consistent with low affinity Na^+/glucose cotransport. In contrast to SGLT1, SGLT2 does not transport D-galactose. By comparing the initial rate of [^{14}C]-αMeGlc uptake with the Na^+-influx calculated from αMeGlc-evoked inward currents, we show that the Na^+ to glucose coupling ratio of SGLT2 is 1:1. Using combined in situ hybridization and immunocytochemistry with tubule segment specific marker antibodies, we demonstrate an extremely high level of SGLT2 message in proximal tubule S1 segments. This level of expression was also evident on Northern blots and likely confers the high capacity of this glucose transport system. We conclude that SGLT2 has properties characteristic of the renal low affinity high capacity Na^+/glucose cotransporter as previously reported for perfused tubule preparations and brush border membrane vesicles. Knowledge of the structural and functional properties of this major renal Na^+/glucose reabsorptive mechanism will advance our understanding of the pathophysiology of renal diseases such as familial renal glycosuria and diabetic renal disorders. (*J. Clin. Invest.* 1994. 93:397–404.) Key words: glucose transport • human kidney • low affinity transport • glycosuria • diabetes

Introduction

Glucose transport across epithelial cells of the kidney proximal tubule and the small intestine is mediated by brush border Na^+-coupled glucose transporters termed SGLT and basolateral facilitated glucose transporters (GLUT)[1] (1, 2). In the mammalian kidney, the major site for glucose reabsorption is the early S1 segment of the proximal convoluted tubule (3). Free-flow micropuncture studies in rat demonstrated that approximately 90% of the filtered glucose is reabsorbed by this tubule segment and only a small fraction of the filtered load reaches the straight tubule of the proximal nephron (second part of the S2 segment and all of the S3 segment; reference 4).

In vitro perfusion studies of rabbit proximal tubules provided evidence for the existence of a low affinity Na^+-coupled glucose transporter in S1 segments and a high affinity Na^+-coupled glucose transporter located in S3 segments (5). In rabbit kidney, the high affinity system corresponds to the high affinity Na^+/glucose cotransporter SGLT1 (6–8) previously cloned from small intestine (9, 10). Although the low affinity system is believed to provide the major renal reabsorptive mechanism for D-glucose the structure of this protein remained unknown.

In vitro perfused tubule studies further demonstrated that the low affinity Na^+/glucose cotransporter has a K_m for D-glucose of 1.64 mM and a maximal transport rate (J_{max}) of 83 pmol/min per mm, whereas the high affinity Na^+/glucose cotransporter has a K_m for D-glucose of 0.35 mM and a J_{max} of only 7.9 pmol/min per mm (5). Other work indicated that D-galactose is a good substrate for the high affinity but not for the low affinity Na^+/glucose cotransporter (11). Glucose uptake studies into brush border membrane vesicles from rabbit and human kidney cortex are in agreement with the existence of two renal Na^+/glucose cotransporters (11–14). The studies provided evidence for a low affinity transporter with a K_m of ~ 6 mM and a high affinity transporter with a K_m of ~ 0.3 mM and demonstrated a Na^+ to glucose stoichiometry of 1:1 for the low affinity Na^+/glucose cotransporter and of 2:1 for the high affinity Na^+/glucose cotransporter.

In human intestine and kidney, the existence of a shared high affinity Na^+/glucose cotransporter and of a second kidney-specific low affinity Na^+/glucose cotransporter is supported by studies of patients with familial intestinal glucose/galactose malabsorption and renal glycosuria (15, 16). Patients with renal glycosuria were found to have impaired renal but not intestinal glucose absorption, whereas patients with intestinal glucose–galactose malabsorption generally also have an associated mild glycosuria. Thus, at least two gene loci must be present in order to explain impaired glucose absorption in these diseases.

In contrast to kidney, the small intestine is thought to have a single, high affinity Na^+/glucose cotransporter (14). By expression cloning with *Xenopus laevis* oocytes we previously isolated a cDNA coding for the high affinity Na^+/glucose co-

Address correspondence to Dr. Matthias A. Hediger, Renal Division, Brigham and Women's Hospital, 75 Francis Street, Boston, MA 02115.

Received for publication 19 May 1993 and in revised form 16 August 1993.

J. Clin. Invest.

0021-9738/94/01/0397/08 $2.00
Volume 93, January 1994, 397–404

1. *Abbreviations used in this paper:* αMeGlc, α-methyl-D-glucopyranoside; GLUT, basolateral facilitated glucose transporters.

transporter SGLT1 (9). SGLT1 has 10 to 12 predicted membrane spanning domains and shows kinetics, stoichiometry, substrate specificity, and inhibition pattern that are consistent with intestinal and renal high affinity Na^+/glucose cotransport (8, 9, 14). Recent studies by Wright and collegues demonstrated that a point mutation of the SGLT1 gene changing aspartic acid 28 to asparagine can cause glucose–galactose malabsorption (17).

In an effort to search for the kidney-specific low affinity Na^+/glucose cotransporter, we have recently isolated by homology screening a human kidney-specific cDNA (Hu14) that codes for an amino acid sequence with 59% identity to that of SGLT1 (18). The Hu14 protein has the same number of putative membrane-spanning domains and a similar predicted secondary structure as SGLT1. Here we report that Hu14 cDNA codes for a low affinity Na^+/glucose cotransporter (SGLT2; reference 19), which has the properties and the pattern of expression in the kidney that are characteristic of previously characterized renal low affinity Na^+/glucose cotransport. We also describe a method to determine the Na^+ to glucose coupling ratio using a combination of electrophysiology and isotopic uptake measurements. The method may be of general value for studies on the stoichiometry of electrogenic transporters.

Methods

Clones. Rabbit SGLT1 cDNA encodes the high affinity Na^+/glucose cotransporter and was previously isolated by expression cloning from small intestine (9). Clone Hu14 contains the SGLT2 EcoRI-insert in pBluescript II, which was isolated by low stringency screening of a human kidney cDNA library using rabbit SGLT1 as a probe (18). R36/R12 (pBluescript II) is a rat homologue of human SGLT2 (Hediger, M., et al., unpublished sequence).

Characterization of SGLT2 by Xenopus oocyte expression. cRNA was in vitro transcribed from clone Hu14 (SGLT2) using T3 RNA polymerase (18). *Xenopus laevis* oocyte expression studies (19) were performed as described previously (20) with minor modifications. Briefly, collagenase-treated and manually defolliculated oocytes were injected with 50 nl of water or cRNA (50 ng/oocyte). Oocytes were incubated in modified Barth's medium (NaCl 88 mM, KCl 1 mM, $Ca(NO_3)_2$ 0.33 mM, $CaCl_2$ 0.41 mM, $MgSO_4$ 0.82 mM, $NaHCO_3$ 2.4 mM, Hepes 10 mM, pH 7.4) supplemented with pyruvate (2.5 mM) and gentamicin (50 μg/ml). The uptake of radiolabeled substrates was measured 5 d after injection. Groups of 6–8 oocytes were incubated for 1 h (or 2 h in some experiments) in 0.75 ml of standard uptake solution (100 mM NaCl, 2 mM KCl, 1 mM $MgCl_2$, 1 mM $CaCl_2$, 10 mM Hepes, 5 mM Tris, pH 7.4) containing 3.0 μCi of radiolabeled substrate and unlabeled substrate to provide the final concentrations indicated in the legends of Figs. 1 and 3. Uptake in the absence of Na^+ or in lowered Na^+-concentration was measured by substituting NaCl with choline chloride.

Measurement of the Na^+ to glucose coupling ratio of SGLT2. Oocytes were injected with Hu14 (SGLT2)- or rabbit SGLT1-cRNA. 5 d after injection, [^{14}C]α-methyl-D-glucopyranoside (αMeGlc) uptake (2 mM for Hu14 or 50 μM for SGLT1) by cRNA-injected oocytes and water-injected controls was measured in standard uptake solution for 1, 3, 5, and 10 min. Immediately after completion of the uptake measurements, electrophysiological experiments were performed using the same batch of cRNA- or water-injected oocytes. The conventional two-microelectrode voltage clamp method (Axoclamp-2A; Axon Instruments, Inc., Foster City, CA) was used (21). The oocytes were bathed in standard uptake solution and the resting membrane potential was monitored after impaling oocytes with the electrodes. For SGLT1 cRNA-injected oocytes the membrane potential was first measured in uptake solution containing 50 μM αMeGlc. After washing with uptake solution without αMeGlc, the oocytes were clamped at this membrane potential. In Hu14 cRNA- or water-injected oocytes, αMeGlc application did not change the membrane potential significantly, so oocytes were clamped at the resting membrane potential measured in the absence of αMeGlc. Inward currents evoked by bath-applied αMeGlc (50 μM for rabbit SGLT1 and 2 mM for Hu14) at the above determined holding potentials were recorded and the values were converted into the rate of net charge flux according to the following equation: Rate of net charge flux (mol/s) = current (A)/F, whereas F is Faraday's constant (9.65×10^4 C/mol). Current–voltage (I–V) relationships were also measured in Hu14 cRNA- and water-injected oocytes. After measuring the αMeGlc-induced current (2 mM) at −60 mV, the oocyte membrane was depolarized or hyperpolarized in 30-mV intervals and, after stabilization of the membrane currents, αMeGlc-evoked currents were consecutively recorded.

Characterization of SGLT2 in COS-7 cells. COS-7 cells were kindly provided by Felix Wettstein, Department of Microbiology and Immunology, University of California, Los Angeles. Tissue culture medium, serum, and antibiotics were obtained from GIBCO (Gaithersburg, MD). The eukaryotic expression vector pEUK-C1 was from Clontech (Palo Alto, CA). Plasmid pEUK-Hu14 was constructed by inserting the 2.26-kb Hu14 cDNA (EcoRI fragment, blunt-ended with T4 DNA polymerase) into the SmaI site of plasmid pEUK-Cl. The orientation and the correct insertion at the 5′-end was confirmed by DNA sequencing. pEUK-Hu14 (15 μg) was transfected into COS-7 cells using Lipofectin as described previously (22). Briefly, cells were seeded onto 35-mm tissue culture plates (Falcon Plastics Co., Cockeysville, MD) incubated at 37°C in DMEM containing 10% FBS and 1% antimycotic (Fungizon; GIBCO) and transfected at a confluency of 80–95%. Before transfection, cell monolayers were washed twice with OPTI-MEM I medium (GIBCO). For each 35-mm plate, 15 μg of plasmid and 15 μg of Lipofectin were mixed for 30 min in 0.5 ml of OPTI-MEM I medium and then added to the plate. After incubation for 24 h at 37°C in a humidified atmosphere containing 5% CO_2, 1 ml of DMEM with 10% serum was added. Uptake studies of αMeGlc were performed 48 to 72 h after transfection. The plates were incubated with choline chloride solution (140 mM choline chloride, 2 mM KCl, 1 mM $CaCl_2$, 1 mM $MgCl_2$, 10 mM Hepes, and 5 mM Tris) for 5 min. Then 0.75 ml of uptake solution containing 2 μCi [^{14}C]αMeGlc per plate, 50 μM αMeGlc (final concentration), 140 mM NaCl, 2 mM KCl, 1 mM $CaCl_2$, 1 mM $MgCl_2$, 10 mM Hepes, and 5 mM Tris was added. After 30 min, the uptake was stopped by aspirating off the uptake solution and rapidly washing the plate with ice-cold washing solution (140 mM choline chloride, 2 mM KCl, 1 mM $CaCl_2$, 1 mM $MgCl_2$, 10 mM Hepes, 5 mM Tris, and 10 mM αMeGlc). The cells were solubilized in 0.2 M NaOH and aliquoted for liquid scintillation counting. The protein concentration was determined using the Bradford dye-binding procedure (23). In control experiments, pEUK-C1 plasmid DNA without insert was transfected. The transfection efficiency was monitored after cotransfection with plasmid pCH110 (Clontech) as described previously (22) and was between 15 and 25%.

In situ hybridization. For these studies, rat kidney tissue was fixed with 4% paraformaldehyde, and 5-μm cryostat sections were cut, as previously described (24). The techniques for in situ hybridization were as described (24) with minor modifications. Briefly, sense and antisense cRNA probes were synthesized from an Hu14 subclone in pBluescript II containing nucleotides 1–973, after linearization with KpnI or EcoR1, using T3 or T7 RNA polymerase, respectively. RNA probes were degraded by partial hydrolysis for 20 min. The slides were washed under medium stringency conditions after hybridization. The washing conditions were the same as reported except that the final washing temperatures (in 5× SSC/10 mM DTT for 30 min and in 2× SSC/10 mM DTT/50% formamide for 20 minutes) were 40°C instead of 50°C. The tissue slides were coated with Kodak NTB2 emulsion and developed 4 wk later. The sections were counter-stained with hematoxylin-eosin. The kidney tubules showing a positive hybridization signal were identified using tubule segment–specific antibodies. The sections adjacent to those used for in situ hybridization were analyzed by immunocytochemistry using the S1 segment–specific anti–GLUT2 anti-

body, the anti-carbonic anhydrase IV antibody, which stained the S2 segment of proximal tubules and thick ascending limbs of Henle's loop, and the S3 segment-specific anti-ecto-ATPase antibody, as described earlier (24). Sections were incubated with the primary antibodies for 1 h at room temperature, and antigenic sites were detected using the ABC procedure as previously described, using diaminobenzidine as a substrate to reveal peroxidase activity (24). The specificity of all antibodies used in this study has been detailed previously (25–27).

Results

Hu14 expressed in oocytes induced a Na^+-dependent uptake of αMeGlc that was 2- to 3.5-fold greater than that of water-injected control oocytes (Fig. 1 *a–c*). D-glucose and αMeGlc were transported equally well, but there was no significant transport of D-galactose, D-fructose, D-mannose, myo-inositol, L-proline, and uridine (Fig. 1 *a*). The substrate specificity was confirmed by inhibition studies (Fig. 1 *b*). [^{14}C]αMeGlc uptake (3 mM) was strongly inhibited by an excess (30 mM) of unlabeled αMeGlc and D-glucose, whereas L-glucose, 3-*O*-methyl-D-glucoside, D-galactose, uridine, and L-proline (not shown) were not efficient inhibitors. Hu14-induced uptake of αMeGlc (2 mM) was phlorizin sensitive (Fig. 1 *c*) and the IC_{50}-value was ~ 1 μM.

Transient expression of Hu14 cDNA in COS-7 cells. This expression system was chosen because it has been useful for studying the properties of the high affinity Na^+/glucose cotransporter SGLT1 (22). Moreover, COS-7 cells are derived from the simian kidney (28) and may synthesize renal mem-

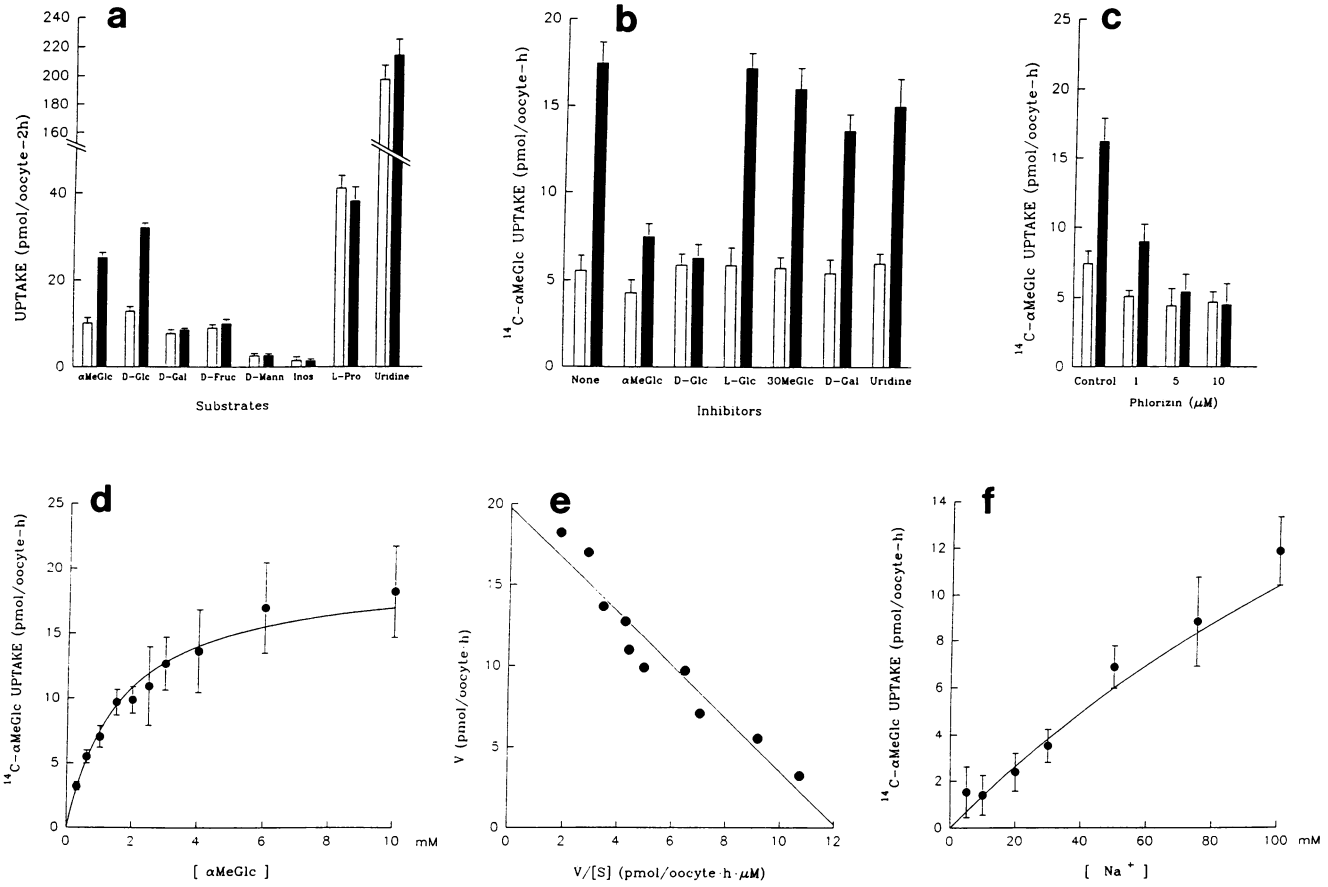

Figure 1. Transport characteristics of Hu14 cRNA-injected *Xenopus laevis* oocytes. (*a*) Substrate specificity of Hu14-mediated transport. Uptake of the radiolabeled substrates αMeGlc, [^{14}C]D-glucose (D-Glc), [^{14}C]D-galactose (D-Gal), [^{14}C]D-fructose (D-fruc), [^{3}H]D-mannose (D-Mann), [^{3}H]myo-inositol (Inos), [^{14}C]L-proline and [^{3}H]uridine were measured in Hu14 cRNA-injected oocytes (*solid bars*) and water-injected control oocytes (*open bars*). Hu14 cRNA-injected oocytes show the uptake of αMeGlc and D-glucose. The concentration of each substrate was 2 mM. (*b*) Inhibition of Hu14-mediated αMeGlc uptake using the substrates as indicated. [^{14}C]αMeGlc (3 mM) uptake was measured in Hu14 cRNA-injected oocytes (*solid bars*) and water-injected oocytes (*open bars*) in the presence of 30 mM of inhibitor and in the absence of inhibitors. The uptake was measured in modified uptake solution containing 85 mM NaCl, 30 mM inhibitors (15 mM choline chloride was added if no inhibitor was used), 2 mM KCl, 1 mM $MgCl_2$, 1 mM $CaCl_2$, 10 mM Hepes, 5 mM Tris, pH 7.4, 30 MeGlc, 3-*O*-methyl-D-glucose. (*c*) Phlorizin inhibition. [^{14}C]αMeGlc (2 mM) uptake in the Hu14 cRNA-injected oocytes (*solid bars*) and water-injected oocytes (*open bars*) was measured in the presence and absence of phlorizin. (*d*) Concentration dependence of αMeGlc. Uptakes of [^{14}C]αMeGlc between 0.3–10 mM was measured in Hu14 cRNA-injected oocytes, subtracted with the uptake obtained from water-injected oocytes and plotted. The curve was fitted using the Michaelis–Menton equation. (*e*) Eadie–Hofstee plot of Hu14-mediated αMeGlc uptake from d. The K_m and V_{max} values are 1.6 mM and 19.7 pmol/oocyte per h, respectively. (*f*) Na^+-dependency of Hu14-mediated αMeGlc uptake. [^{14}C]αMeGlc uptake (2 mM) was measured at various Na^+ concentrations (0–100 mM) in Hu14 cRNA-injected oocytes, and the uptake measured in water-injected oocytes was subtracted. Uptake values were plotted against the Na^+ concentration and the curve fitted using the Michaelis–Menton equation. Error bars represent SEMs (n = 6–8).

brane proteins more efficiently than amphibian oocytes. In test experiments we expressed high affinity SGLT1. We show a 240-fold stimulation of the uptake of [^{14}C]αMeGlc (50 μM) compared to cells transfected with control plasmid (Fig. 2 *a*). This is consistent with the several hundredfold stimulation observed for rabbit SGLT1 expressed in oocytes (9, 14). By analogy with the expression studies of Hu14 using oocytes, cells transfected with Hu14-plasmid DNA exhibited an approximately twofold increase of Na^+-dependent and phlorizin sensitive sugar uptake (50 μM αMeGlc) compared to cells transfected with control plasmid (Fig. 2 *a* and *b*). These experiments confirm the observation from oocytes that Hu14 cDNA induces Na^+-dependent sugar uptake and indicate that the relatively low level of uptake of SGLT2 (see Fig. 1 *d*) in oocytes is not due to aberrant protein biosynthesis in the amphibian expression system.

Kinetic properties of Hu14-induced αMeGlc uptake in oocytes. The saturation of αMeGlc uptake in Hu14 cRNA-injected oocytes is demonstrated in Fig. 1 *d*. Based on Eadie–Hofstee plot analysis (Fig. 1 *e*) the K_m value for αMeGlc is 1.6 mM. Hill plot analysis based on the data in Fig. 1 *d* gave a Hill coefficient of 1.1 (not shown), indicating that there is one glucose binding site per transporter molecule.

The Na^+-dependency of αMeGlc uptake in Hu14 cRNA-injected oocytes was examined by measuring the uptake of [^{14}C]αMeGlc (2 mM) as a function of the sodium concentration in the uptake medium (Fig. 1 *f*). αMeGlc uptake did not saturate at Na^+ concentrations between 5 and 100 mM, indicating that the K_m value for Na^+ is considerably larger than 100 mM.

Comparison with previously determined kinetic parameters. The K_m of 1.6 mM for αMeGlc uptake mediated by the Hu14 protein (SGLT2) is almost identical to the K_m of 1.64 mM for D-glucose uptake for the rabbit kidney low affinity Na^+/glucose transporter as determined based on in vitro perfused tubule studies (5). In contrast, a K_m value for low affinity D-glucose uptake into cortical brush border membrane vesicles of ~ 6 mM was reported (11, 13). A possible explanation of this discrepancy is that these vesicle studies were carried out at lower concentration of Na^+ (40 mM). Previous studies of high affinity SGLT1 revealed that the K_m for αMeGlc is substantially larger at lower Na^+-concentrations (40).

Based on our results, SGLT2 most likely corresponds to the previously characterized low affinity Na^+/glucose cotransporter from kidney outer cortex (5, 11, 13). The K_m for Na^+ of SGLT2 is also considerably larger than the $K_{0.5}$ (the Na^+ concentration giving half the value of V_{max}) of high affinity SGLT1, which is 32 mM (14). This demonstrates the different Na^+-dependencies between these two transporters. Lineweaver–Burk analysis using the data in Fig. 1 *f* suggested that the K_m value for Na^+ for SGLT2 is between 250 and 300 mM (not shown). This range is in agreement with the high K_m value for Na^+ reported for the low affinity Na^+/glucose cotransporter of rabbit brush border membrane vesicles, which is 228 mM at 1 mM of D-glucose (29).

Stoichiometry of SGLT2. Since the K_m for Na^+ of SGLT2 is considerably higher than the physiological concentration of Na^+ for oocytes, which is ~ 100 mM, the Hill coefficient and the Na^+ to glucose coupling ratio calculated based on Na^+-concentrations significantly below the K_m may underestimate the stoichiometry. Therefore, it was essential to compare directly the rate of αMeGlc influx with the rate of Na^+ influx. First, we attempted to compare the [^{14}C]αMeGlc uptake with the $^{22}Na^+$ uptake but, because of the low signal-to-noise ratio for $^{22}Na^+$ uptake, we were unable to measure the Na^+-influx.

To circumvent these problems, we measured the αMeGlc-induced Na^+-dependent inward current as an indicator for the Na^+-influx and converted the current amplitude to the rate of Na^+ influx. The Hu14-mediated αMeGlc-induced inward current was completely Na^+-dependent (not shown). The strategy was to compare the initial rate of [^{14}C]αMeGlc uptake with that of the Na^+-influx calculated from the αMeGlc-evoked inward current. The same batch of oocytes was used for these two experiments. Because the Hu14-mediated current was dependent on membrane voltage (Fig. 3 *a*) the holding potential was set at the resting membrane potential of each oocyte. The average resting membrane potential was −70.4±1.5 mV (mean±SEM, n = 8) in water-injected oocytes and −68.5±2.5 mV (mean±SEM, n = 11) in Hu14 cRNA-injected oocytes. The inward current evoked by 2 mM of αMeGlc was 0.90±0.09 nA (n = 11) for Hu14 cRNA-injected oocytes and 0.44±0.03 nA (n = 8) for water-injected oocytes. Using Faraday's constant, these currents were converted to 9.3 and 4.5 fmol/s, respectively. It follows that the initial rate of the net Na^+-flux mediated by SGLT2 is 4.8 fmol/s or 0.29 pmol/min per oocyte (Fig. 3 *c*). This was compared to the 1-min uptake of [^{14}C]αMeGlc (2 mM), which is 0.31 pmol/oocyte per min (Fig. 3 *b* and *c*) and in this respect the 1-min uptake can be considered as representative for the initial rate since the uptake was almost linear within the first 5 min. Based on the similar αMeGlc- and Na^+-uptake rates, it can be concluded that the Na^+ to glucose coupling ratio for SGLT2 is 1:1. This is consistent with the Hill coefficients of ~ 0.9 for Na^+ (calculated based on the data presented in Fig. 1 *f*) and of 1.1 for αMeGlc.

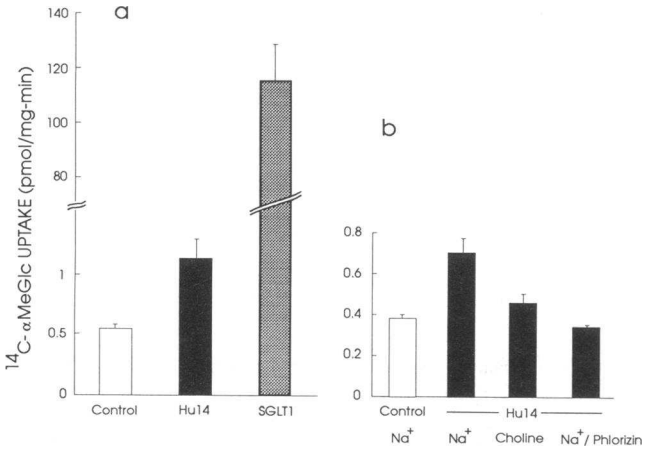

Figure 2. Expression of Hu14 in Cos-7 cells. (*a*) [^{14}C]αMeGlc (50 μM) uptake was measured in COS-7 cells transfected with control plasmid, Hu14, or rabbit SGLT1. Rabbit SGLT1 transfected COS-7 cells showed a 240-fold stimulation of [^{14}C]αMeGlc uptake, whereas Hu14-transfected cells showed approximately a twofold stimulation of uptake compared to control plasmid-transfected COS-7 cells. (*b*) Na^+-dependency and phlorizin sensitivity of [^{14}C]αMeGlc uptake in Hu14-transfected COS-7 cells. αMeGlc uptake induced by Hu14 cDNA was suppressed in Na^+-free uptake solution (indicated by "choline") or in uptake solution containing 100 μM phlorizin. The error bars represent the standard SEMs (n = 3).

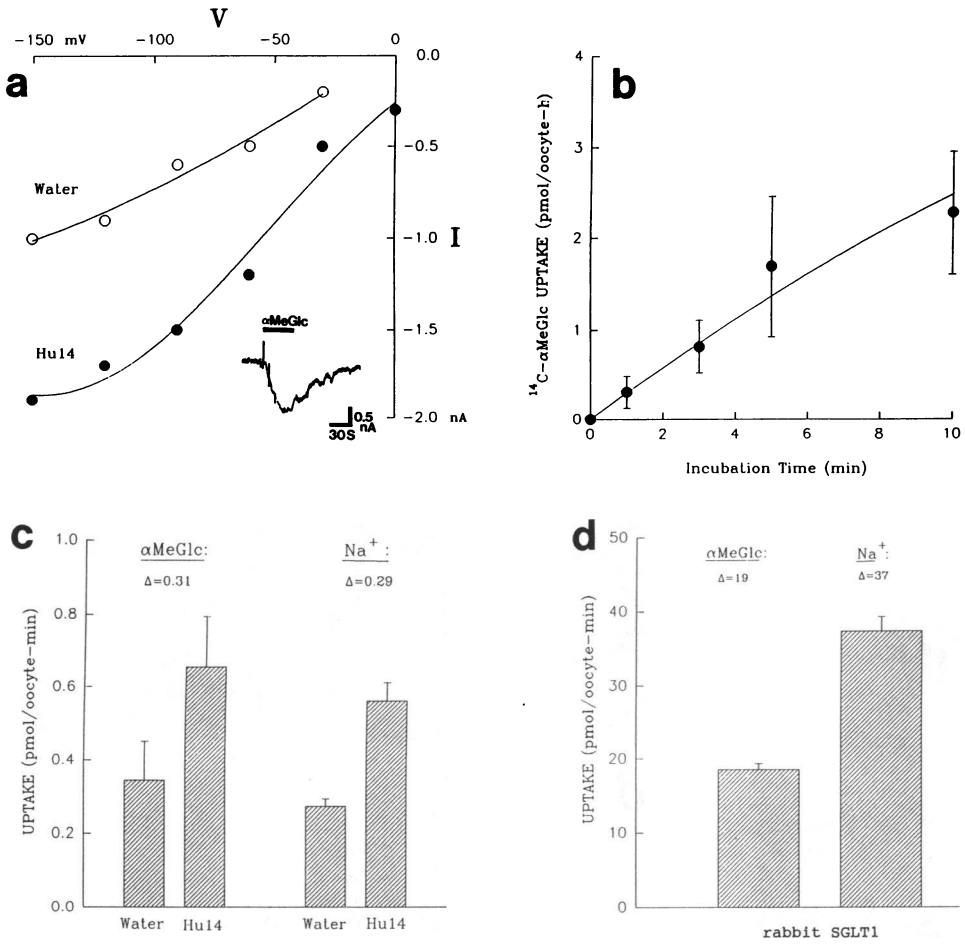

Figure 3. Stoichiometric analysis of Hu14-mediated transport. (*a*) Representative current–voltage (*I–V*) relationship of αMeGlc-induced responses (2 mM) in Hu14 cRNA-injected oocytes (*closed circles*) and water-injected oocytes (*open circles*). The inset shows a representative αMeGlc-induced inward current in Hu14 cRNA-injected oocytes. (*b*) Time course of Hu14-mediated [^{14}C]αMeGlc uptake (2 mM). Uptake was measured for 1, 3, 5, and 10 min and subtracted from that of water-injected oocytes. (*c*) Comparison of [^{14}C]αMeGlc uptake and Na^+ influxes. The left panel shows the [^{14}C]αMeGlc uptakes in oocytes injected with water or Hu14 cRNA. The Hu14-mediated αMeGlc uptake was, after subtraction from that of water injected oocytes, 0.31 pmol/oocyte per min. The right panel shows Na^+-influx in water-injected oocytes and Hu14 cRNA-injected oocytes. The Hu14-mediated Na^+-influx was, after subtracting that of water-injected oocytes, 0.29 pmol/oocyte per min. The experiment demonstrates that the Na^+/glucose coupling ratio of SGLT2 is 1:1. (*d*) Determination of the Na^+/glucose coupling ratio of rabbit SGLT1 using the same procedure as in *c*. The figure shows the uptake of [^{14}C]-αMeGlc and Na^+ in rabbit SGLT1 expressed in oocytes. Uptake in water-injected control oocytes is not shown because this was negligible compared with that induced by SGLT1. The initial rate of αMeGlc uptake was 19 pmol/oocyte per h and that of Na^+ influx was 37 pmol/oocyte per h. This confirms that the Na^+/glucose coupling ratio of SGLT1 is 2:1. The error bars represent SEMs (n = 6–8 for ^{14}C-uptake measurements and 8–11 for electrophysiologal measurements).

A ratio of 1 Na^+ to 1 glucose is also consistent with the stoichiometric analysis of low affinity Na^+/glucose cotransport in renal outer cortex brush border membrane vesicles (12, 29).

The reliability and accuracy of the stoichiometric analysis method was confirmed using oocytes injected with rabbit SGLT1-cRNA (Fig. 3 *d*). Previous Hill plot analysis of the Na^+-dependent αMeGlc uptake of SGLT1 demonstrated a Hill coefficient of 1.5 (14), indicating a Na^+ to glucose coupling ratio of 2:1. Since application of 50 μM αMeGlc significantly depolarized the SGLT1 cRNA-injected oocyte membrane, from a resting potential of −52.8±2.1 mV (n = 9) to −17.4±1.7 mV (n = 9) in the presence of 50 μM αMeGlc, it was necessary for our stoichiometric analysis to hold the membrane potential at the potential measured in the presence of 50 μM αMeGlc. The Na^+-influx induced by 50 μM of αMeGlc was calculated to be 37±2.1 pmol/oocyte per min (n = 9; Fig. 3 *d*). The 1-min [^{14}C]αMeGlc uptake was within the linear range of uptake and was 19±0.8 pmol/oocyte per min (n = 8). The Na^+ to glucose coupling ratio for SGLT1 is therefore 2:1, consistent with the studies of SGLT1 expressed in oocytes (14) and with the known stoichiometry of the high affinity Na^+/glucose cotransport in brush border membrane vesicles (12, 30, 31).

Localization of SGLT2 in the kidney tubular system. In previous studies we demonstrated that Hu14 mRNA is expressed strongly in human kidney cortex but not in the small intestine or in any other rat tissue tested (18), whereas the SGLT1 mRNA is strongly expressed in the intestine (10, 18). Northern analysis has not yet resulted in the detection of SGLT1 message in the human kidney, but has demonstrated a low level of expression in rat and rabbit kidney (6–8, 18). The localization of SGLT2 mRNA in the kidney was studied using in situ hybridization. Hybridization of ^{35}S-labeled Hu14-antisense cRNA probe to rat paraformaldehyde-fixed kidney sections under medium stringency conditions (Fig. 4) demonstrated a pattern of hybridization that is consistent with the predicted location of the low affinity Na^+/glucose cotransporter in proximal tubule S1 segments (Fig. 4 *a*). The location in S1 segments was confirmed using adjacent sections in which the positive tubules reacted with the S1 segment–specific marker antibody against the low affinity facilitated glucose transporter GLUT2, as noted in (25), (Fig. 4 *c*). By contrast, no significant Hu14 signal was detected in tubules that were immunopositive for the anti-carbonic anhydrase type IV antibody, which stains S2 segments of proximal tubules and thick ascending limbs of Henle, as noted in (26), (Fig. 4 *d*), and the

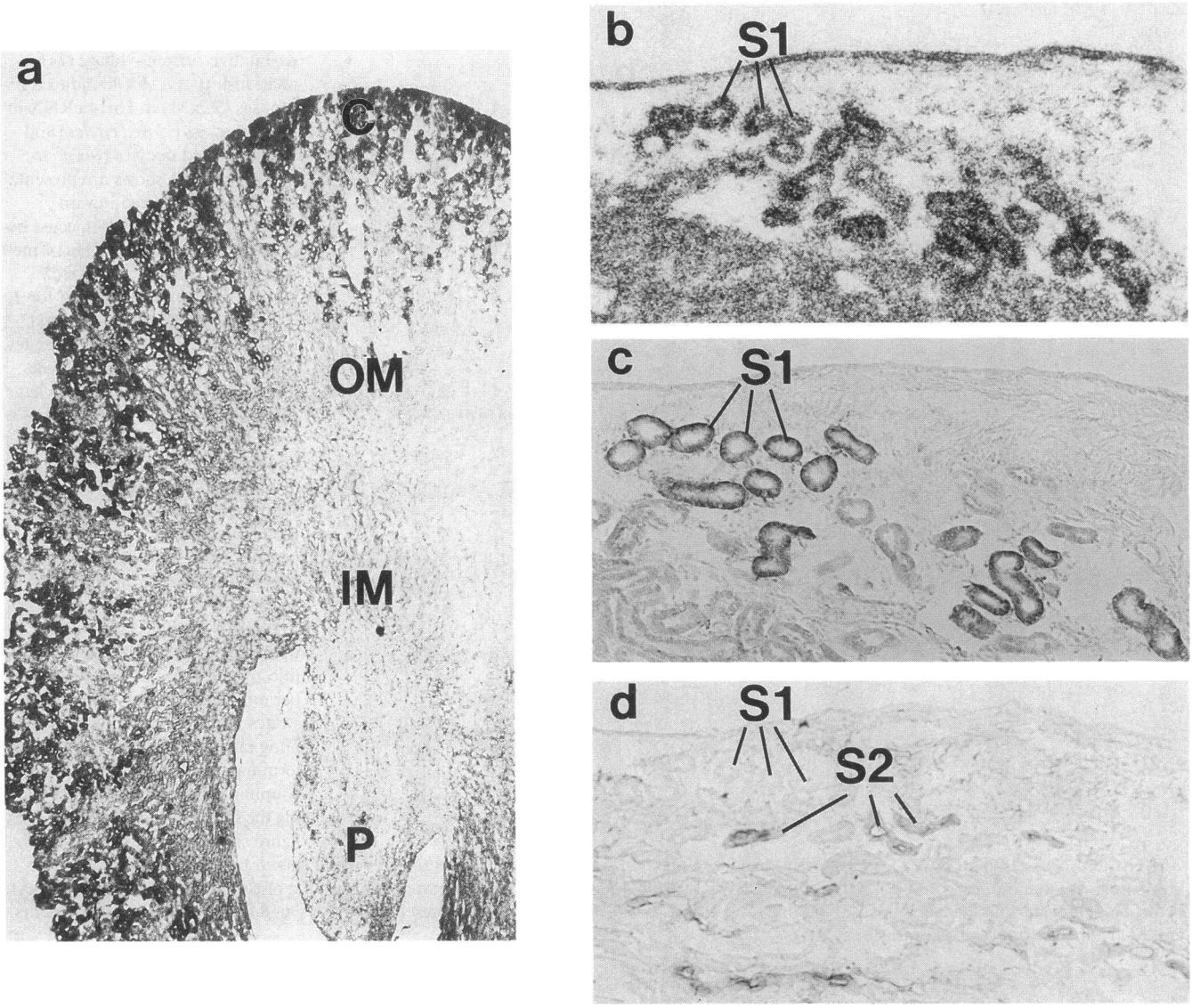

Figure 4. Localization of SGLT2 message in the kidney tubules by in situ hybridization. (*a*) Low power micrograph showing the pattern of hybridization of Hu14 antisense cRNA probe (^{35}S-labeled) to rat kidney cryosections. A strong hybridization is detected over tubules in the cortex (*C*), whereas the signal is absent in outer medulla (*OM*), inner medulla (*IM*), and papilla (*P*). (*b–d*) Sequential 5 μm sections of rat kidney cortex hybridized with Hu14 antisense cRNA probe (*b*) or stained with antibodies against the S1 segment specific marker GLUT2 (*c*) or carbonic anhydrase IV (*d*), which is specific for S2 segments of proximal tubules and the thick ascending limbs of Henle's loop. A strong hybridization signal is evident in *b* and is localized over tubules that show a basolateral staining for GLUT2 (indicated as S1 in *c*). In contrast, carbonic anhydrase IV positive tubules (indicated as S2 in *d*) do not contain a Hu14 hybridization signal. The S3 segment-specific anti–ecto-ATPase antibody did not stain tubules in the field corresponding to *b* and ecto-ATPase-positive tubules detected in other areas of the kidney did not contain Hu14 hybridization signal (not shown). Bar, 0.4 mm (*a*) and 0.1 mm (*b–d*).

S3-specific anti–ecto-ATPase antibody, as noted in (27), (not shown). An identical pattern of expression was also obtained using ^{35}S-labeled antisense cRNA of the rat SGLT2 homologue R36/R12 (unpublished sequence) at a considerably higher hybridization stringency (Hediger, M. A., et al., unpublished data). We conclude, therefore, that kidney-specific low affinity SGLT2 is expressed in S1 proximal tubule segments where the majority of filtered glucose is absorbed. All properties of SGLT2 determined so far are consistent with those of the kidney-specific low affinity/high capacity Na^+-glucose cotransport system, which has been characterized in the past by studies using perfused tubule segments and using brush border membrane vesicles (5, 8, 11, 12, 29).

Comparison of the properties of SGLT2 and SGLT1 expressed in Xenopus oocytes. In oocytes, the apparent V_{max} of Hu14 of 19.7 pmol/oocyte per h, which was determined in the presence of 100 mM Na^+ (Fig. 1, *d* and *e*) is substantially lower than that of SGLT1, which is 150–1,550 pmol/oocyte per h (14). Likewise, Hu14-mediated uptake of αMeGlc was increased 2–3.5-fold above control values, whereas a stimulation of several hundredfold was observed for SGLT1 in oocytes (9, 14). This difference may be explained in part by the higher K_m

for Na^+ (250–300 mM) for SGLT2 compared to the $K_{0.5}$ of SGLT1, which is 32 mM (14). At an extracellular Na^+ concentration of 100 mM, the Na^+ drive of SGLT2 is, based on the Michaelis–Menton equation, only ~ 27% of V_{max}, whereas the Na^+ drive of SGLT1 is, based on the Hill equation, 90% of V_{max}.

The low V_{max} of SGLT2 compared with SGLT1 may, furthermore, be related to the turnover rate of the transporter. Based on pre-steady-state currents measured electrophysiologically, Wright and colleagues estimated the turnover rate of SGLT1 in oocytes to be 57/s (32). This is substantially faster than that of the GABA transporter, which is 6–13/s as determined by Lester and co-workers using the same procedure (33). A lower turnover rate of SGLT2 compared with SGLT1 would significantly contribute to the low V_{max} of the transporter. Finally, differences in the density of functional SGLT1 and SGLT2 carriers in the oocytes' plasma membrane could also account for the difference in V_{max}.

SGLT2 as a low affinity/high capacity system in renal proximal tubules. In the kidney, the low affinity Na^+/glucose transport system of the pars convoluta of proximal tubules (S1 segments) is known to be a high capacity system and the majority of D-glucose must be reabsorbed in this part of the tubule (4). Consistent with this, brush border membrane vesicles prepared from outer cortex have about a 3.4-fold higher Na^+/glucose transport capacity than those from the outer medulla (8). As discussed above, the V_{max} of SGLT2 expressed in oocytes, however, is less than that of SGLT1. Therefore, for SGLT2 to represent a high capacity system in vivo, the expression of this protein must be accordingly high. Consistent with this, we observed a very strong signal for SGLT2 on Northern blots of rat tissues, whereas the signal for SGLT1 was near the detection limit (see reference 18, Fig. 5, 4.2-kb band for SGLT1 in medulla, 2.4-kb band for SGLT2 in cortex). The strong signal for SGLT2 compared with SGLT1 was also evident in our in situ hybridization experiments using rat SGLT1 and SGLT2 cRNA as probes (Hediger M. A., et al., unpublished data).

It appears reasonable that the coupling of one Na^+ per glucose of low affinity SGLT2 is sufficient to drive the absorption of the bulk of the D-glucose in the early proximal tubule of the kidney where the glucose concentration is high. In contrast, the coupling of two Na^+ per glucose provides a substantially higher accumulative power for the high affinity Na^+/glucose cotransporter SGLT1 located in proximal tubule S3 segments. This high accumulative power is necessary to absorb the last traces of D-glucose from the lumen of S3 segments into the blood (1, 34).

SGLT2 and renal disorders. Elsas and Rosenberg proposed that at least two gene loci are necessary to explain the impaired glucose absorption in glucose/galactose malabsorption and renal glycosuria (15, 16). Consistent with this, the genes that encode high affinity SGLT1 and the low affinity SGLT2 reside on different genes located on different chromosomes: SGLT1 resides on chromosome 22q13.1 (32, 35) and we recently demonstrated that SGLT2 is located on chromosome 16 close to the centromere (41). Based on the localization of SGLT2 in the kidney it is conceivable that a defect of the SGLT2 gene is responsible for impaired glucose reabsorption in patients with renal glycosuria. Interestingly, galactose, which is a substrate of high affinity SGLT1, was not transported by SGLT2. This is consistent with in vitro perfused tubule studies of the low affinity Na^+/glucose cotransporter in rabbit kidney (11). Examination of renal excretion of galactose, therefore, may provide useful information to distinguish between defects in SGLT1 and SGLT2.

Previous studies suggested that increased Na^+/glucose reabsorption in diabetes may have important implications in the development of renal hypertrophy (36). It has been proposed that increased proximal Na^+ reabsorption causes cell growth in the proximal tubule, increases glomerular filtration rate (GFR), and is at least in part responsible for the development of nephropathy (37, 38). Other investigators hypothesize that enhanced glucose reabsorption accelerates irreversible glycosylation of tissue proteins (39). The elucidation of the structural and functional properties of the major renal glucose reabsorptive mechanism may provide important insights into these pathologic changes of the kidney in diabetes.

Acknowledgments

We are grateful to Steven Hebert for stimulating discussions, and to Paula Boutin for technical assistance.

This work was supported by the National Institutes of Health through grants DK-43632 and DK-43171 to M. A. Hediger, and DK-42956 to D. Brown, respectively, the International Human Frontier Science Program Organization Long-Term Fellowship to Y. Kanai, and the Juvenile Diabetes Foundation International to W-S. Lee.

References

1. Silverman, M., and R. J. Turner. 1992. Glucose transport in the renal proximal tubule. *In Handbook of Physiology, Section 8: Renal Physiology, Vol. 2, E. E. Windhager, editor. Oxford University Press, Oxford.* 2017–2038.

2. Schafer, J. A., and J. C. Williams, Jr. 1985. Transport of metabolic substrates by the proximal nephron. *Annu. Rev. Physiol.* 47:103–125.

3. Berry, C. A., and F. C. Rector, Jr. 1991. Renal transport of glucose, amino acids, sodium, chloride, and water. In The Kidney. 4th. Ed. B. M. Brenner and F. C. Rector, Jr., editors. W.B. Saunders Co., Philadelphia. 245–282.

4. Rector, F. C., Jr. 1983. Sodium, bicarbonate, and chloride absorption by the proximal tubule. *Am. J. Physiol.* 244:F461–F471.

5. Barfuss, D. W., and J. A. Schafer. 1981. Differences in active and passive glucose transport along the proximal nephron. *Am. J. Physiol.* 240:F322–F332.

6. Coady, M. J., A. M. Pajor, and E. M. Wright. 1990. Sequence homologies among intestinal and renal Na^+/glucose cotransporters. *Am. J. Physiol.* 259:C605–C610.

7. Morrison, A. I., M. Panayotova-Heiermann, G. Fiegl, B. Scholermann, and R. K. Kinne. 1991. Sequence comparison of the sodium-D-glucose cotransport systems in rabbit renal and intestinal epithelia. *Biochim. Biophys. Acta.* 1089:121–123.

8. Pajor, A. M., B. A. Hirayama, and E. M. Wright. 1992. Molecular evidence for two renal Na^+/glucose cotransporters. *Biochim. Biophys. Acta.* 1106:216–220.

9. Hediger, M. A., M. J. Coady, T. S. Ikeda, and E. M. Wright. 1987. Expression cloning and cDNA sequencing of the Na^+/glucose cotransport. *Nature (Lond.).* 330:370–381.

10. Hediger, M. A., E. Turk, and E. M. Wright. 1989. Homology of the human intestinal Na^+/glucose and Escherichia coli Na^+/proline cotransporters. *Proc. Natl. Acad. Sci. USA.* 86:5748–5752.

11. Turner, R. J., and A. Moran. 1982. Heterogeneity of sodium-dependent D-glucose transport sites along the proximal tubule: evidence from vesicle studies. *Am. J. Physiol.* 242:F406–F414.

12. Turner, R. J., and A. Moran. 1982. Further studies of proximal tubular brush border membrane D-glucose transport heterogeneity. *J. Membr. Biol.* 70:37–45.

13. Turner, R. J., and M. Silverman. 1977. Sugar uptake into brush border vesicles from normal human kidney. *Proc. Natl. Acad. Sci. USA.* 74:2825–2829.

14. Ikeda, T. S., E. S. Hwang, M. J. Coady, B. A. Hirayama, M. A. Hediger, and E. M. Wright. 1989. Characterization of a Na^+/glucose cotransporter cloned from rabbit small intestine. *J. Membr. Biol.* 110:87–95.

15. Elsas, L. J., R. E. Hillman, J. H. Patterson, and L. E. Rosenberg. 1970. Renal and intestinal hexose transport in familial glucose-galactose malabsorption. *J. Clin. Invest.* 49:576–585.

16. Elsas, L. J., and L. E. Rosenberg. 1969. Familial renal glycosuria: a genetic reappraisal of hexose transport by kidney and intestine. *J. Clin. Invest.* 48:1845–1854.

17. Turk, E., B. Zabel, S. Mundlos, J. Dyer, and E. M. Wright. 1991. Glucose/galactose malabsorption caused by a defect in the Na^+/glucose cotransporter. *Nature (Lond.)*. 350:354–356.

18. Wells, R. G., A. M. Pajor, Y. Kanai, E. Turk, E. M. Wright, and M. A. Hediger. 1992. Cloning of a human kidney cDNA with similarity to the sodium-glucose cotransporter. *Am. J. Physiol.* 263:F459–F465.

19. Hediger, M. A., E. Turk, A. M. Pajor, and E. M. Wright. 1989. Molecular genetics of the human Na^+/glucose cotransporter. *Klin. Wochenschr.* 67:843–846.

20. Hediger, M. A., T. Ikeda, M. Coady, C. B. Gundersen, and E. M. Wright. 1987. Expression of size-selected mRNA encoding the intestinal Na^+/glucose cotransporter in *Xenopus* oocytes. *Proc. Natl. Acad. Sci. USA.* 84:2634–2637.

21. Kanai, Y., and M. A. Hediger. 1992. Primary structure and functional characterization of a high-affinity glutamate transporter. *Nature (Lond.)*. 360:467–471.

22. Birnir, B., H. S. Lee, M. A. Hediger, and E. M. Wright. 1990. Expression and characterization of the intestinal Na^+/glucose cotransporter in COS-7 cells. *Biochim. Biophys. Acta.* 1048:100–104.

23. Bradford, M. M. 1976. A rapid and sensitive method for quantitation of microgram quantities of protein utilizing the principle of protein-dye binding. *Anal. Biochem.* 72:248–254.

24. Kanai, Y., M. G. Stelzner, W.-S. Lee, R. G. Wells, D. Brown, and M. A. Hediger. 1992. Expression of mRNA (D2) encoding a protein involved in amino acid transport in S3 proximal tubule. *Am. J. Physiol.* 263:F1087–F1092.

25. Thorens, B., H. J. Lodish, and D. Brown. 1990. Differential localization of two glucose transporter isomforms in rat kidney. *Am. J. Physiol.* 259:C286–C294.

26. Brown, D., X. L. Zhu, and W. S. Sly. 1990. Localization of membrane-associated carbonic anhydrase type IV in kidney epithelial cells. *Proc. Natl. Acad. Sci. USA.* 87:7457–7461.

27. Sabolic, I., O. Culic, S.-H. Lin, and D. Brown. 1992. Localization of ecto-ATPase in rat kidney and isolated renal cortical membrane vesicles. *Am. J. Physiol.* 262:F217–F228.

28. Gluzman, Y. 1981. SV40-transformed simian cells support the replication of early SV40 mutants. *Cell.* 23:175–182.

29. Turner, R. J., and A. Moran. 1982. Stoichiometric studies of the renal outer cortical brush border membrane D-glucose transporter. *J. Membr. Biol.* 67:73–80.

30. Kimmich, G. A., and J. Randles. 1984. Sodium–sugar coupling stoichiometry in chick intestinal cells. *Am. J. Physiol.* 247:C74–C82.

31. Restrepo, D., and G. A. Kimmich. 1985. Kinetic analysis of mechanism of intestinal Na^+-dependent sugar transport. *Am. J. Physiol.* 248:C498–C509.

32. Loo, D. D. F., A. Hazama, S. Supplisson, E. Turk, and E. M. Wright. 1993. Relaxation kinetics of the Na^+/glucose cotransporter. *Proc. Natl. Acad. Sci. USA.* 90:5767–5771.

33. Mager, S., J. Naeve, M. Quick, C. Labarca, N. Davidson, and H. A. Lester. 1993. Steady states, charge movements, and rates for a cloned GABA transporter expressed in Xenopus oocytes. *Neuron.* 10:177–188.

34. Turner, R. J. 1985. Stoichiometry of co-transport systems. *Annu. NY Acad. Sci.* 456:10–25.

35. Hediger, M. A., M. L. Budarf, B. S. Emanuel, T. K. Mohandas, and E. M. Wright. 1989. Assignment of the human intestinal Na^+/glucose cotransporter gene (SGLT1) to the q11.2→qter region of chromosome 22. *Genomics.* 4:297–300.

36. Carney, S. L., N. L. M. Wong, and J. H. Dirks. 1979. Acute effects of streptozotocin diabetes on rat renal function. *J. Lab. Clin. Med.* 93:950–962.

37. Kumar, A. K., R. K. Gupta, and A. Spitzer. 1988. Intracellular sodium in proximal tubules of diabetic rats. Role of glucose. *Kidney Int.* 33:792–797.

38. Hannedouche, T. P., A. G. Delgado, D. D. Gnionsahe, C. B. Boitard, B. Lacour, and J.-P. Grunfeld. 1990. Renal hemodynamics and segmental tubular reabsorption in early type I diabetes. *Kidney Int.* 37:1126–1133.

39. Brownlee, M., A. Cerami, and H. Vlassara. 1988. Advanced glycosylation end products in tissue and the biochemical basis of diabetic complications. *N. Engl. J. Med.* 318:1315–1321.

40. Parent, L., S. Supplisson, D. D. F. Loo, and E. M. Wright. 1992. Electrogenic properties of the cloned Na^+/glucose cotransporter: I. Voltage-clamp studies. *J. Membr. Biol.* 125:49–62.

41. Wells, R. G., T. K. Mohandas, and M. A. Hediger. 1993. Localization of the Na^+/glucose cotransporter gene SGLT2 to human chromosome 16 close to the centromere. *Genomics.* 17:787–789.